# A Water Soluble Macromolecular Nanobox Having Porphyrinic Walls as a Large Host for Giant Guests

**Placido Mineo,[1,2] Fabiola Spitaleri,[1] Emilio Scamporrino[1]**

[1]Dipartimento di Scienze Chimiche and I.N.S.T.M. UdR of Catania, Università di Catania, Viale A. Doria, 6, 95125 Catania, Italy
[2]CNR-IPCF Istituto per i Processi Chimico Fisici, Viale Ferdinando Stagno D'Alcontres, 37, 98158 Messina, Italy
Correspondence to: P. Mineo (E-mail: gmineo@unict.it)

Received 1 October 2012; accepted 28 November 2012; published online 7 January 2013
**DOI: 10.1002/pola.26515**

**ABSTRACT**: Cyclic tetra{5,15-di-[*p*($\omega$-methoxypolyethyleneoxy)-phenyl]-10,20-[*p*-oxyphenyl] methylen porphyrin}, **cy-[O-($H_2$-PTPEG$_2$)-O-$CH_2$-]$_4$**, a water soluble macromolecule consisting of four porphyrin units [each with two long $\omega$-methoxypolyethyleneoxy (PEG) branches bound on its peripheral positions] linked by means of four methylenoxy bridges, was prepared by an interfacial etherification reaction. Structural and spectroscopic characterization of cy-[O-($H_2$-PTPEG$_2$)-O-$CH_2$-]$_4$ and of its cobalt-derivative {cy-[O-(Co-PTPEG$_2$)-O-$CH_2$-]$_4$} was performed by means of MALDI-TOF mass spectrometry, NMR, UV–vis, and circular dichroism spectroscopy. The data obtained from the cy-[O-(Co-PTPEG$_2$)-O-$CH_2$-]$_4$/Gramicidin-S mixture showed that some evident spectral changes were compatible with the formation of a supramolecular structure between the porphyrinic nanobox and the Gramicidin S (a polypeptide having a relevant pharmacological importance). These preliminary data highlight how cy-[O-($H_2$-PTPEG$_2$)-O-$CH_2$-]$_4$ and/or its metalled derivatives, for their both chemical composition and structural arrangement, have promising properties for applications as a drug carrier in aqueous media. © 2013 Wiley Periodicals, Inc. J. Polym. Sci., Part A: Polym. Chem. **2013**, *51*, 1428–1435

**KEYWORDS**: host-guest systems; hydrophilic polymers; MALDI; polyethers; sensors; star polymers

**INTRODUCTION** In the last years, the biomedical research has had to deal with complex problems related to the increased incidence of cancerous pathologies as a consequence of an increment of the average life and of the exposition to environments increasingly polluted.

Efforts in this field are pharmacological oriented towards the development of "smart molecules" able to selectively recognize the diseased cells on which to act.[1a] The strategies until now followed concern the use of molecules with suitable cavities in their structure where to insert the drug molecules with pharmacological activity.[1b]

Generally, for larger drug molecules vesicular systems are used. They are often complex aggregates systems consisting of amphiphilic species that tend to form, in aqueous environment, micellar structures in which the active drug molecules may be trapped.[2–5]

Unfortunately, with these systems, the drug is however, brought indiscriminately throughout the body, and released, often without any specific control, in all tissues and also in healthy cells. Moreover, the amphiphilic material (present in large excess with respect to the amount of the drug) is metabolized by the body with the possible occurrence of an acute or chronic toxicity so that alternative more functional strategies are searched.

All this has led to the development of new molecular systems that can: (i) recognize the target molecules; (ii) be, in turn, a potential drug; (iii) be analytically determinable; and (iv) carry specific drugs, releasing them only where necessary.

For their peculiar properties, excellent candidates to satisfy the first three points are the porphyrin compounds. However, as a negative aspect, the marked hydrophobic nature of the heteromacrocycle core is, unfortunately, responsible of a strong insolubility of these compounds in aqueous media. In some cases, by the inclusion of ionic groups in the porphyrin structure the insolubility has been mitigated[6–8] without substantially change the affinity for the DNA molecules, but often the electric interaction with the cell membranes prevents their crossing.[9]

Recently, some of these water-soluble porphyrins have been tested in important applications such as the treatment of transmissible spongiform encephalopathy (known as the bovine variant "mad cow disease"), in chemotherapy and in photodynamic therapy.[10–13]

Additional Supporting Information may be found in the online version of this article.

However, another problem concerns the drug release from the porphyrin complexes. In fact, porphyrin systems and, in particular, their metal derivatives, easily form supramolecular complexes with suitable electron-rich bio-molecules (as amino acids and drugs) but more complicated is their controlled release and only a few studies concerning this problem are in literature.

Recently, as a first step of a work in this topic, we have synthesized some cyclic formal-porphyrin oligomers,[14] soluble in organic solvents. Now, in this work we have designed a simple and fast procedure to synthesize uncharged water soluble macromolecular nanobox. In particular, we report the synthesis of cyclic tetra{5,15-di-[p($\omega$-methoxypolyethyleneoxy) phenyl]-10,20-[p-oxyphenyl]methylen porphyrin}, (indicated in the followed as **cy-[O-($H_2$-PTPEG$_2$)-O-C$H_2$-]$_4$**) which, having a 3D structure with four porphyrin units held together by ether formal bridges, forms as a molecular box. Besides the synthesis, chemical and spectroscopic characterization of this cyclic *tetra*-porphyrin-ether (and its Cobalt derivative {cy-[O-(Co-PTPEG$_2$)-O-C$H_2$-]$_4$}) by means of MALDI-TOF mass spectrometry, NMR, UV–vis spectroscopy, and circular dichroism, is here reported. Preliminary data about the formation of complexes with Gramicidin S (a polypeptide having a relevant pharmacological importance) are also discussed.

## EXPERIMENTAL

### Materials

All the solvents and basic materials were commercial products appropriately purified before use.

### UV-Visible and Circular Dichroism

UV–visible spectra were recorded at room temperature by a Shimadzu Model 1601 spectrophotometer, in quartz cells, using tetrahydrofurane (THF) or $H_2O$ as a solvent. Circular dichroism measurements were performed on a Jasco J815 spectropolarimeter at $T = 25.0 \pm 0.1$°C.

### $^1$H-NMR Analyses

$^1$H-NMR, COSY, and T-ROESY spectra were obtained on a UNITY INOVA Varian instrument operating at 500 MHz ($^1$H) using VNMR for software acquisition and processing. Samples were dissolved in $CD_2Cl_2$ and the chemical shifts expressed in ppm by comparison with the $CH_2Cl_2$ residue signal. The spectra were acquired at 27°C, with a spin lock time of 0.5 s. COSY and T-ROESY spectra were acquired using a Varian standard impulse sequence. In the T-ROESY experiment, a spin lock field of 2000 Hz with a spin lock time of 0.5 s were applied.

### MALDI-TOF Mass Spectrometric Analysis

Positive MALDI-TOF mass spectra were acquired by a Voyager DE-STR (PerSeptive Biosystem) using a simultaneous delay extraction procedure (25 kV applied after 2600 ns with a potential gradient of 454 V mm$^{-1}$ and a wire voltage of 25 V) and detection in linear mode.[15,16]

The instrument was equipped with a nitrogen laser (emission at 337 nm for 3 ns) and a flash AD converter (time base 2 ns). Trans-3-indoleacrylic acid (IAA) was used as a matrix. Mass spectrometer calibration and average molecular mass determination were performed as reported in previous cases.[17–19]

Each m/z value reported in the spectra and in the text is referred to the ion containing the most abundant isotope of each element present in the molecule.

### Synthesis of Tetrakis-(*p*-hydroxyphenyl)porphyrin, $H_2$-P(OH)$_4$

This product was prepared according to the method described by Little et al.,[20] starting from pyrrole and *p*-acetoxybenzaldehyde in boiling propionic acid.

### Synthesis of 5,15-Di-[*p*($\omega$-methoxypolyethyleneoxy)phenyl]-10,20-[*p*-hydroxyphenyl] Porphyrin, HO($H_2$-PTPEG$_2$)OH

HO($H_2$-PTPEG$_2$)OH was obtained by reaction between $\omega$-methoxypolyethyleneoxy chloride [PEGMEC, having an average $M_w = 750$ Da (MWD = 1.05) and formed by reaction between poly(ethyleneglycol)methyl ether (PEGME) and thionyl chloride in THF] and **$H_2$-P(OH)$_4$**.[21]

Briefly, 2.625 g of PEGMEC (3.5 mmol) dissolved in 10 mL of a $H_2O$/THF (1/1) mixture, 0.298 g of **$H_2$-P(OH)$_4$** (0.44 mmol) dissolved in 35 mL of a 0.5*M* NaOH aqueous solution was added and the mixture refluxed for 24 h. Further 10 mL of 0.5*M* NaOH and 10 mL of THF were then added and the solution refluxed for other 24 h.

When, examining aliquots of the mixture, the conversion in di-(*p*-hydroxyphenyl)porphyrin, considering the relative amount of the cluster of molecular ion peaks centered at about m/z 2200 in the MALDI-TOF spectrum (see Fig. 1) with respect to the clusters of other derivatives[21] was judged optimal, the solution was slightly acidified with $CH_3COOH$, dried under vacuum and the residue dissolved in $CH_2Cl_2$, filtered and fractionated by column chromatography by using silica gel as stationary phase and a solution of $CH_2Cl_2$/EtOH/N($C_2H_5$)$_3$ (96.5/2.0/1.5) as an eluent. By MALDI-TOF-MS (Fig. 2), $^1$H-NMR, COSY, and ROESY experiments, the third

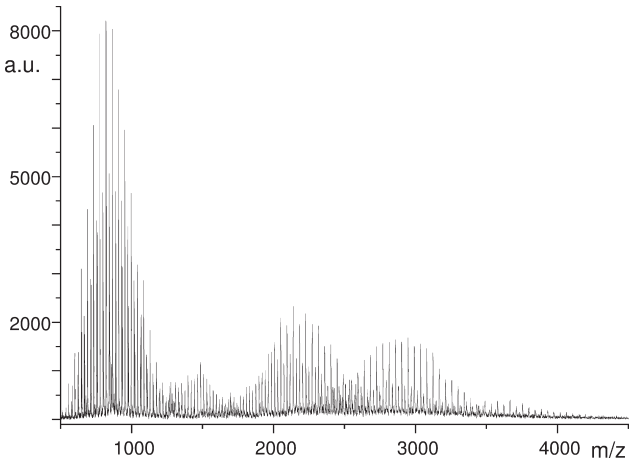


**FIGURE 1** MALDI-TOF spectra of the reaction product between PEGMEC and tetrakis-(*p*-hydroxyphenyl) porphyrin.

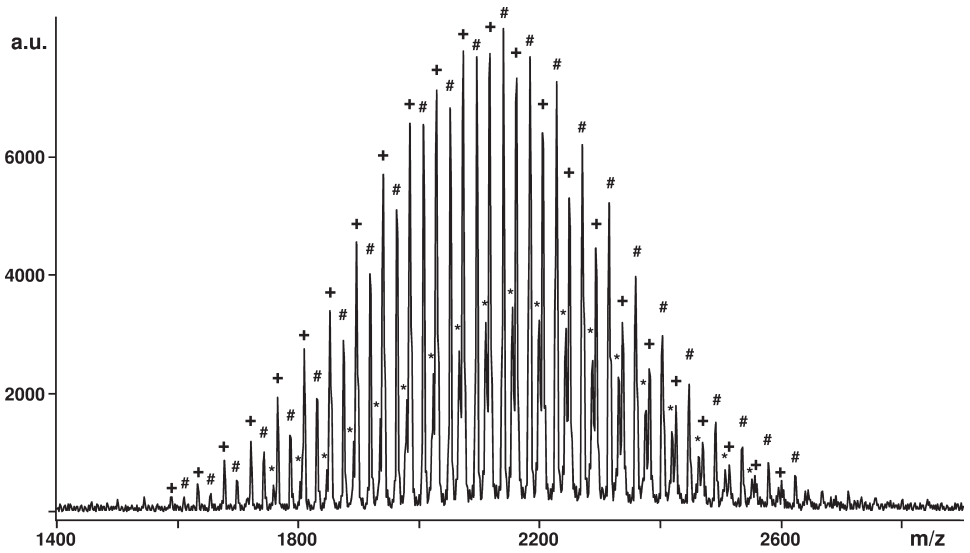


**FIGURE 2** MALDI-TOF mass spectrum of HO($H_2$-PTPEG$_2$)OH.

compound eluted from the column (collected with a yield of 13% with respect to the initial porphyrin amount) resulted pure **HO($H_2$-PTPEG$_2$)OH**.

Its $^1$H-NMR spectrum (500 MHz, in $CD_2Cl_2$ at 27°C; for the atom identification see inset of Fig. 3) showed the following signals: two unresolved doublets at 8.87 ppm (4 H, pyrrole protons 2, 8, 12, 18) and 8.70 ppm (4 H, pyrrole protons 3, 7, 13, 17); a doublet at 8.01 ppm (4 H, phenyl protons **a**′); a broad signal at 7.8 ppm (4 H, phenyl protons **a**); a doublet at 7.27 (4 H, CH phenyl protons **b**′); a broad signal at 6.96 (4 H, CH phenyl protons **b**); a broad triplet at 4.12 ppm (4 H, methylene protons **c**); a broad triplet at 3.89 ppm (4 H, methylene protons **d**); some broad signals in the range 3.75–3.55 ppm (128 H, PEO methylene protons); a singlet at 3.46 ppm (6 H, terminal methyl groups $\omega$); a singlet (not shown) at −2.86 ppm (2H, N—H pyrrole protons 21, 22).

Instead, the fourth compound eluted from the column (collected with a yield of 28% with respect to the initial porphyrin amount) resulted the 5,10-di-[*p*($\omega$-methoxypolyethyleneoxy)phenyl]-15,20-[*p*-hydroxyphenyl]porphyrin, **HO($H_2$-PCPEG$_2$)OH** (see Supporting Information for its $^1$H-NMR characterization data).

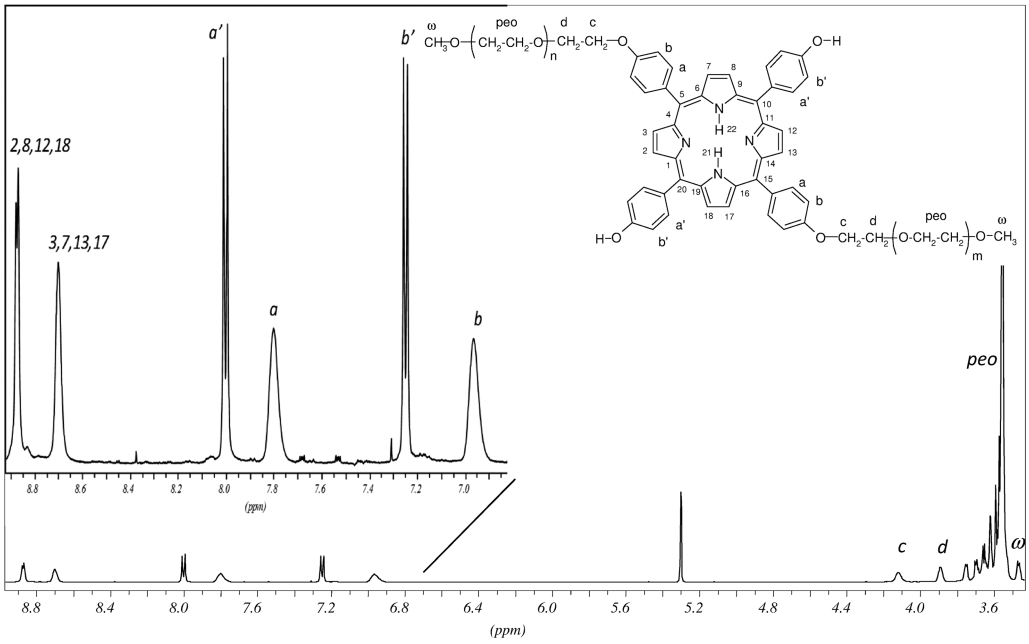


**FIGURE 3** $^1$H-NMR of HO($H_2$-PTPEG$_2$)OH. In the inset, structure of HO($H_2$-PTPEG$_2$)OH and NMR assignments.

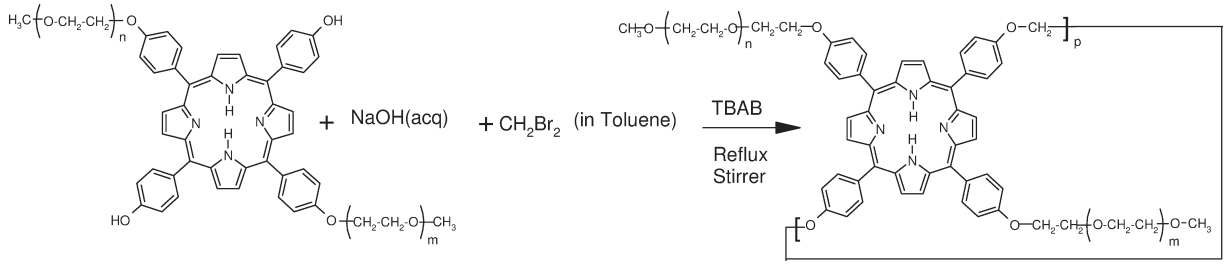


**SCHEME 1** Synthesis of *tetra*{5,15-di-[*p*($\omega$-methoxypolyethyleneoxy)phenyl]-10,20-[*p*-oxyphenyl] methylen porphyrin}, cy-[O-($H_2$-PTPEG$_2$)-O-$CH_2$-]$_4$.

### Synthesis of Cyclic *Tetra*{5,15-di-[*p*($\omega$-methoxypolyethyleneoxy)phenyl]-10,20-[*p*-oxyphenyl] Methylen Porphyrin}, cy-[O-($H_2$-PTPEG$_2$)-O-$CH_2$-]$_4$

Cyclic-ethers, having methylene bridges between the porphyrin units, were synthesized by interfacial etherification reaction in toluene/$H_2O$ between **HO($H_2$-PTPEG$_2$)OH** and a large excess of dibromomethane with tetrabutyl ammoniumbromide (TBAB) used as phase-transfer agent (Scheme 1).

In a typical synthetic procedure (see Scheme 1), to 200 mg of **HO($H_2$-PTPEG$_2$)OH** (ca. 0.095 mmol), dissolved in 100 mL of a 2*M* NaOH solution, 230 mg of TBAB (0.7 mmol) was added at room temperature. Then, a solution of 10 mL of $CH_2Br_2$ in 80 mL of toluene was added and the mixture refluxed under vigorous stirring, monitoring the reaction by TLC chromatography, and MALDI-TOF mass spectrometry. After 24 h, the reaction was stopped and the material contained in the organic phase recovered by rotoevaporation in vacuum. From the mixtures of oligomers (yield of 90% with respect to the initial **HO($H_2$-PTPEG$_2$)OH** amount), the pure cy-[O-($H_2$-PTPEG$_2$)-O-$CH_2$-]$_4$ was collected by column chromatography, using silica gel as stationary phase and a $CHCl_3$/MeOH/N($C_2H_5$)$_3$ (97.5/2.0/0.5) mixture as eluant (yield of 18%).

In particular, its $^1$H-NMR (500 MHz, in $CD_2Cl_2$ at 27°C; for the atom identification see Figure SI3 in Supporting Information) showed: some broad signals in the range 9.10–8.67 ppm (32 H, C—H pyrrole protons) and 8.45–8.01 ppm (32 H, phenyl protons); two broad signals at 7.70 and 7.34 ppm (32 H, phenyl protons); a broad signal at 6.34 ppm (8 H, methyleneoxy protons); some broad signals between 4.78 and 3.23 ppm (544 H, methylene protons of PEO); a singlet at 3.18 ppm (24 H, methyloxy protons); a singlet at −2.71 ppm (8H, N—H pyrrole protons).

### Preparation of the Cyclic *tetra*{5,15-di-[*p*($\omega$-methoxypolyethyleneoxy)phenyl]-10,20-[*p*-oxyphenyl] Methylene-cobalt-porphyrin}, cy-[O-(Co-PTPEG$_2$)-O-$CH_2$-]$_4$

The insertion of cobalt ions, by substitution of the two hydrogen atoms in each porphyrin core of Cy-[O-($H_2$-PTPEG$_2$)-O-$CH_2$-]$_4$ was obtained by reaction of this last with a large molar excess (1:10) of cobalt acetate in pyridine at 100°C under a $N_2$ atmosphere. Pure cy-[O-(Co-PTPEG$_2$)-O-$CH_2$-]$_4$ was recovered by chromatographic separation using silica gel as stationary phase and a $CHCl_3$/$C_2H_5OH$/N($C_2H_5$)$_3$ (96,5/2,0/1,5) mixture as eluent (yield of almost 100%).

## RESULTS AND DISCUSSION

The synthesis of cyclic-ether oligomers containing porphyrin units involved the use of **HO($H_2$-PTPEG$_2$)OH** in turn obtained by the reaction between **$H_2$-P(OH)$_4$** and $\omega$-methyloxy polyethyleneoxy chloride. As expected, from this last reaction, a mixture of porphyrin derivatives with a different number of polyethylenoxy branches was obtained.

In fact, the MALDI-TOF spectrum of the obtained product resulted constituted of five clusters of peaks (see Fig. 1): the cluster centered at about m/z 800 was due to the unreacted PEGMEC; the cluster centered at about m/z 1400 corresponded to the oligomers of the mono-branched porphyrin derivatives {the 5-[*p*-($\omega$-methoxy-polyethylenoxy)phenyl]-10,15,20-tri–(*p*-hydroxyphenyl) porphyrin}; the cluster centered at about m/z 2200 was due to the mixture of the two di-branched porphyrin isomers {**HO($H_2$-PTPEG$_2$)OH** and the 5,10-di-[*p*-($\omega$-methoxy-polyethylenoxy)phenyl]-15,20-di–(*p*-hydroxyphenyl)porphyrin}; the cluster centered at about m/z 2900 was due to the tri-branched porphyrin oligomers {the 5,10,15-tri-[*p*-($\omega$-methoxy-polyethylenoxy)phenyl]-20-(*p*-hydroxyphenyl)porphyrin}; the last cluster centered at about m/z 3600 was due to the *tetra*-branched porphyrin derivative.

Pure **HO($H_2$-PTPEG$_2$)OH** was obtained by chromatographic fractionation and, on the basis of its MALDI-TOF mass spectrum and some marked characteristics of its NMR spectra, **HO($H_2$-PTPEG$_2$)OH** resulted the third eluted product. Figure 2 shows its MALDI-TOF mass spectrum consisting in a single cluster of peaks (ca. 1600–2700 Da), centered at about m/z 2100 (ca. $M_n$ = 2090, MWD = 1.04) with a separation of the peaks of 44 amu as a consequence of the different total number of oxyethylene units in the two PEG branches. In particular, each molecular ion with a $n + m$ value between 0 and 25 (see structure in the inset of Fig. 3) appears as $M_{n+m}H^+$ (peaks at m/z 1587 + n44, indicated as "+"), $M_{n+m}Na^+$ (peaks at m/z 1609+ n44, indicated as "#") and $M_{n+m}K^+$ (peaks at m/z 1625+ n44, indicated as "*") species.

The exact identification of **HO($H_2$-PTPEG$_2$)OH** as the center-symmetrical 10,20-di[*p*-hydroxyphenyl]porphyrin isomer, was achieved by the NMR analysis (see Experimental section

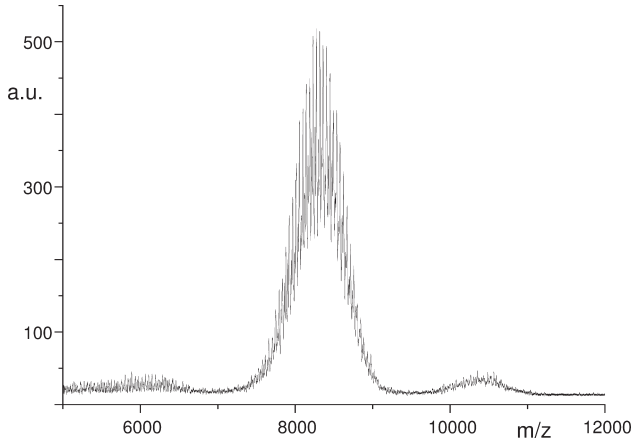


**FIGURE 4** MALDI-TOF mass spectrum of oligo[5,15-di-[*p*($\omega$-methoxy-polyethyleneoxy)phenyl]-10,20-[*p*-oxyphenyl] methylen porphyrin].

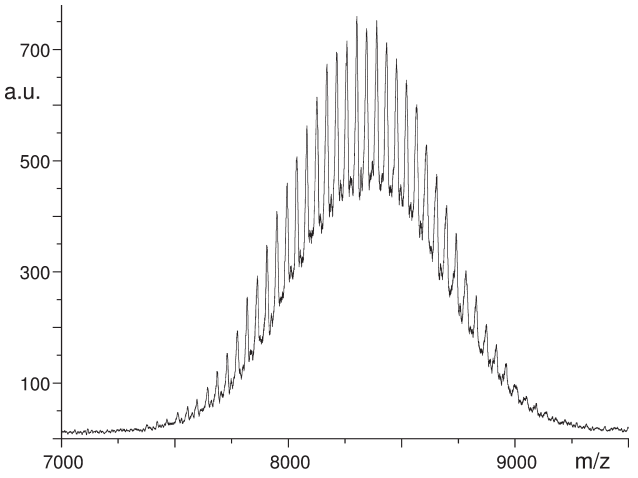


**FIGURE 5** MALDI-TOF mass spectrum of cycle(*tetra*[5,15-di-[*p*($\omega$-methoxy-polyethyleneoxy) phenyl]-10,20-[*p*-hydroxyphenyl] methylen porphyrin]).

and Fig. 3). The structural assignment was also supported by T-ROESY and COSY experiments (see Supporting Information) which showed, respectively, the diagnostic cross-peak correlations between protons **c** and **b**; **a** and (3, 7)-(13, 17) and **a**′ and (2,18)-(8, 12) and between the signals of the **a**-**b**, **a**′-**b**′, and **c-d** protons.

To enhance the formation of cyclic oligomers, the subsequent condensation reaction between HO($H_2$-PTPEG$_2$)OH and dibromomethane, was performed in diluted condition (for more details see Experimental section).

Figure 4 shows the MALDI-TOF mass spectrum of the oligomers mixture, which consists of several clusters of peaks corresponding to the molecular ions of cyclic cy-[O-($H_2$-PTPEG$_2$)-O-$CH_2$-]$_n$ oligomers with a different number of repetitive units ($p$ = 3–5, see Scheme 1). As expected, the higher intensity of the signals of the cluster relative to the cyclic tetra-ether oligomer (centered at ca. 8400), indicated this as the most abundant species formed in the reaction.

Pure cy-[O-($H_2$-PTPEG$_2$)-O-$CH_2$-]$_4$ was then obtained by chromatographic column fractionation with a yield of 18%. Its MALDI-TOF spectrum, reported in Figures 5, showed peaks at m/z: 7537 + n44, between about m/z 7500 to m/z 9200, with $n$ = 0–36, corresponding to molecular ions detected as $MH^+$.

The chemical structure of cy-[O-($H_2$-PTPEG$_2$)-O-$CH_2$-]$_4$ was also confirmed by NMR analysis (see Supporting Information). In particular, the signal at 6.34 ppm was indicative of the ether linkage formation[14] between the porphyrins. Moreover, the spectrum of the cyclic tetramer showed, with respect to that of the **HO($H_2$-PTPEG$_2$)OH,** a broadening of the NMR signals due to both the oligomeric structure of the tetramer and the different conformations of the macro-cycle.

The synthetic procedure ended with the transformation of a part of cy-[O-($H_2$-PTPEG$_2$)-O-$CH_2$-]$_4$ in the corresponding cobalt derivative (cy-[O-(Co-PTPEG$_2$)-O-$CH_2$-]$_4$) by reaction with cobalt acetate. The substitution of the eight pyrrole protons with four $Co^{++}$ was confirmed by the shift of about 230 amu of the peak signals observed in its MALDI-TOF spectrum (Fig. 6) with respect the signals of Figure 5.

The UV–vis spectra of cy-[O-($H_2$-PTPEG$_2$)-O-$CH_2$-]$_4$ in THF (continuous line) and in water (continuous line in the inset) solutions are shown in Figure 7; they exhibited the characteristic intense Soret-band ($\lambda_{max}$ = 425 nm in THF and 424 nm in water) and four satellite Q-bands (between 500 and 700 nm). It particular, the spectrum in THF resulted very similar to that of the starting HO($H_2$-PTPEG$_2$)OH (Fig. 7, dotted line; $\lambda_{max}$ = 421 nm in THF). Instead, the Soret band profile of HO($H_2$-PTPEG$_2$)OH in aqueous solution (see inset Fig. 7, dotted line) clearly shows the energy shifts of the nearly degenerate monomer band, originated from the formation of H-type (band at ca. 400 nm) and, mainly, J-type (band at ca. 442 nm) aggregates.[22,23] This phenomenon, as discussed in our recent works,[22,23] is due to the balance between the hydrophobic interactions and the hydrogen bonding contribution that determining the formation of J- or H-type aggregates.

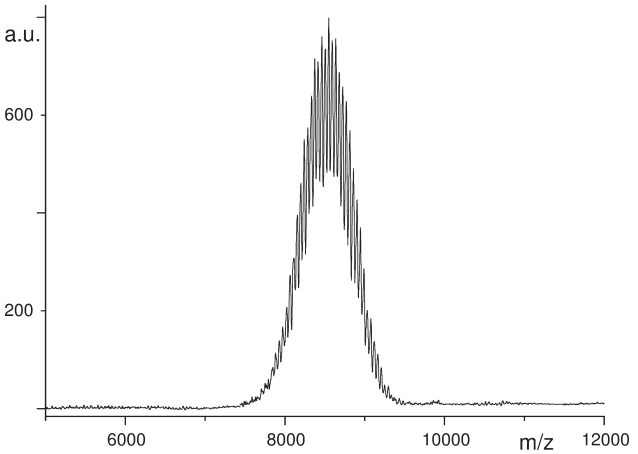


**FIGURE 6** MALDI-TOF spectrum of cy-[O-(Co-PTPEG$_2$)-O-$CH_2$-]$_4$.

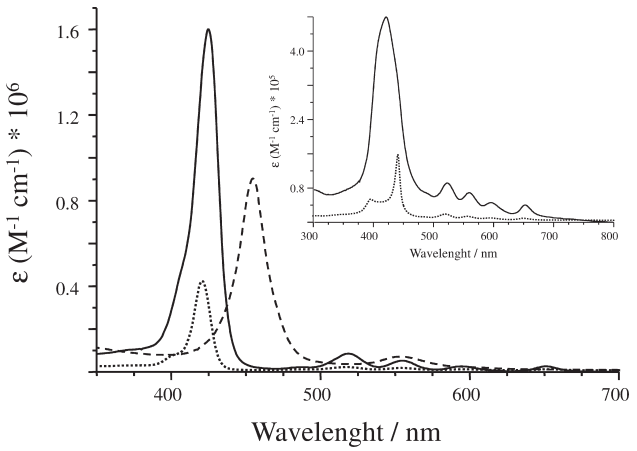


**FIGURE 7** UV–vis spectra of solutions in THF of cy-[O-($H_2$-PTPEG$_2$)-O-$CH_2$-]$_4$ (continuous line), HO($H_2$-PTPEG$_2$)OH (dotted line), and cy-[O-(Co-PTPEG$_2$)-O-$CH_2$-]$_4$ (dashed line). In the inset, UV–vis spectrum of aqueous solution of cy-[O-($H_2$-PTPEG$_2$)- O-$CH_2$-]$_4$ (continuous line) and HO($H_2$-PTPEG$_2$)OH (dotted line).

Differently, the UV–vis spectrum of the cy-[O-(Co-PTPEG$_2$)-O-$CH_2$-]$_4$ in THF solution (dashed line of Fig. 7) showed the typical feature of a metalled porphyrin derivative, with relevant changes in the position (a red shift) and intensity of the Soret band and the disappearance of two Q-bands.

The decreased Q-band number was interpreted on the basis of the already reported so-called "four-orbital model"[24] that describes the low-lying ($\pi$, $\pi^*$) excited states of porphyrins in terms of electronic transitions between the two topmost filled molecular orbitals (HOMO's), $a_{2u}$ ($\pi$) and $a_{1u}$ ($\pi$), to two degenerate lowest empty molecular orbitals (LUMO's), $e_g$ ($\pi^*$). According to this model, metallo-porphyrins should show only two visible Q-bands instead of the four Q-bands shown by the free-porphyrin base.

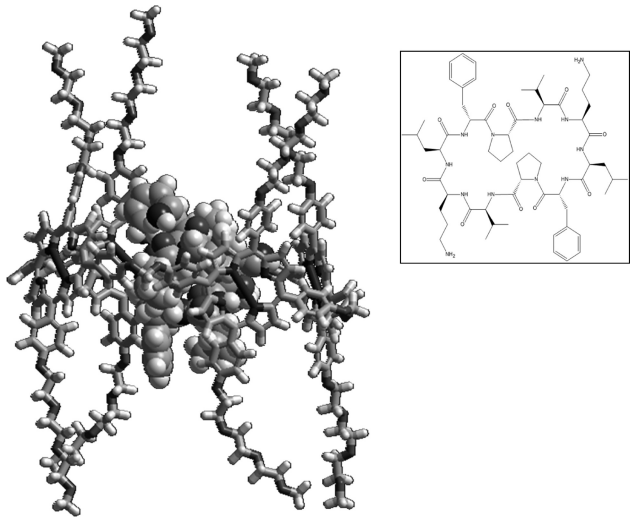

**FIGURE 8** Sketch 3D of the host/guest complex. In the inset, chemical structure of Gramicidin S.

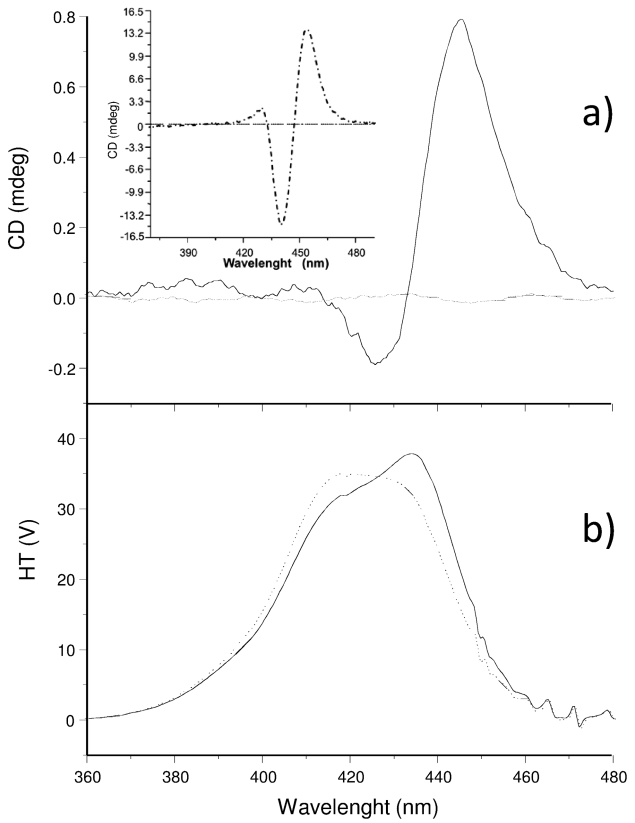


**FIGURE 9** (a) ICD and (b) HT spectra of cy-[O-(Co-PTPEG$_2$)-O-$CH_2$-]$_4$ (concentration 5 $\times 10^{-7}$ M, dotted line) and its mixtures with Gramicidin S (continuous line) in water solution (molar ratio 1:100). In the inset, ICD spectra of Co-P/Gramicidin/Co-P complex[23] (concentration 6 $\times 10^{-6}$ M).

To test the ability of cy-[O-($H_2$-PTPEG$_2$)-O-$CH_2$-]$_4$ and cy-[O-(Co-PTPEG$_2$)-O-$CH_2$-]$_4$ to entrap polypeptide compounds, experiments with Gramicidin S were performed. Besides its well-known antibiotic properties, the choice fell on this cyclic decapeptide [constituted of two identical series of five AAs: (Val, Orn, Leu, D-Phe, and Pro)$_2$] for its molecular size suitable for its possible accommodation into the cyclic-ether cavity (see inset of Fig. 8).

As expected, considering the marked ability of cobalt-porphyrin derivatives to complex AAs residue,[21,25,26] significant results were obtained with cy-[O-(Co-PTPEG$_2$)-O-$CH_2$-]$_4$.

The Soret regions of the high tension voltage (HT, which is roughly proportional to absorbance) and of the CD spectra of freshly prepared aqueous solutions (5 $\times$ $10^{-7}$ M) of pure cy-[O-(Co-PTPEG$_2$)-O-$CH_2$-]$_4$ (dashed line) and its mixture with Gramicidin S (1:100) (continuous line) are compared in Figure 9. Differently from the trace in organic solvent (dashed line in Fig. 6) the Soret band of cy-[O-(Co-PTPEG$_2$)-O-$CH_2$-]$_4$ in water solution [dashed line in Fig. 9(b)] consisted of two overlapped signals of comparable intensity with $\lambda_{max}$ values, respectively, at about 415 and 430 nm. As previously explained in similar cases,[21] these absorptions can be ascribed to the equilibrium between free cy-[O-(Co-PTPEG$_2$)-

O-$CH_2$-]$_4$ molecules and their complex species with a different number of ligands ($H_2O$, —OH, etc.) bound to the metal atoms in axial positions with respect to the porphyrin planes.

The presence of Gramicidin S caused a slight shift of $\lambda_{max}$ of the two band [continuous line spectrum in Fig. 9(b)], respectively, at 420 and 438 nm, which appeared also with a different intensity.

Because cy-[O-(Co-PTPEG$_2$)-O-$CH_2$-]$_4$ is an achiral compound, as expected, no signal was observed in its CD spectrum [dashed line in Fig. 9(a)] whereas an induced circular dichroism (ICD) trace, consisting of an asymmetrical bisigned signal appearing in correspondence with the Soret absorption band, was observed in its aqueous solution with Gramicidin S [molar ratio 1:100; continuous curve of Fig. 9(a)]. The symmetry breaking of the molecular species was considered a strong confirmation of the formation of stable complexes between cy-[O-(Co-PTPEG$_2$)-O-$CH_2$-]$_4$ and Gramicidin S molecules.

Furthermore, by comparison between CD and absorption spectra, it was also possible assigned the HT signal centered at 415 nm in the spectrum of pure cy-[O-(Co-PTPEG$_2$)-O-$CH_2$-]$_4$ [dashed line in Fig. 9(b)], to the free molecules because no ICD signal was observed in its correspondence. Otherwise, the two different ICD signals centered at 428 nm (negative signal) and 448 nm (positive signal) were considered, as in previous similar cases,[21,25,26] indicative of two diverse cy-[O-(Co-PTPEG$_2$)-O-$CH_2$-]$_4$/GramicidinS complexes; probably, by the overlap of the corresponding ICD signals could originate the asymmetry of the bands observed in Figure 9(a).

To put in evidence the effect of the spatial geometry of the macromolecular box in the interaction with Gramicidin S, a new experiment was performed using a mono-porphyrin system, the 5,10,15,20-tetrakis-*p*-($\omega$-methoxypolyethyleneoxyphenyl)-Cobalt-porphyrin[23] (Co-P, a porphyrin with four PEG branches bound in the peripheral position). The ICD spectrum of the Co-P/Gramicidin solution, consisting in a strong [$\Delta$CD ca. 29 mdeg; where $\Delta CD = CD_{453} - CD_{440}$] and almost symmetrical bisigned signal, is reported in the inset of Figure 9. It can be considered that among the AAs of the Gramicidin only Phe (by $\pi$–$\pi$ interactions) and Orn (by interaction between its $\delta$-amino group and the Cobalt atom) could be able to interact with Co-P.

According to a previous work,[26] it can be assumed that two Co-P molecules (by means of the Co atom) are fixed on the Gramicidin surface in correspondence of the two Orn units (by interaction with the AA amine groups) to form a Co-P/Gramicidin/Co-P sandwich complex.

In this way, considering the small size of the Gramicidin (with a Orn-$NH_2$ distance ca. 7.89 Å), the two Co-P units would be close enough in the space to induce (by their electronic mutual interaction) the excitonic coupling phenomenon responsible of the bisigned ICD signals shown in the inset of Figure 9. Instead, in the case of the cyclic tetramer, the ICD signal (Fig. 9) showed a partial asymmetric profile because the appositive box's walls, for the quadrate geometry, are at wide distance (ca. 21.2 Å) to allow an efficacy excitonic coupling.[27] Moreover, also the mutual arrangement of the adjacent perpendicular porphyrins do not allow an efficacy excitonic coupling.[27,28]

## CONCLUSIONS

In summary, we here report the synthesis and the chemical and spectroscopic characterization of a novel water soluble cyclic tetra-ether porphyrin, cy-[O-($H_2$-PTPEG$_2$)-O-$CH_2$-]$_4$, having a molecular architecture similar to a nanobox, and of its Cobalt derivative cy-[O-(Co-PTPEG$_2$)-O-$CH_2$-]$_4$. Remarkably, CD experiments on a mixture in water solution of this last and Gramicidin S showed the formation of supramolecular structures.

Really, the ICD signal was little intense, probably for the low amount of cy-[O-(Co-PTPEG$_2$)-O-$CH_2$-]$_4$/Gramicidin S complex species formed, but sufficient enough to observe the phenomenon. However, in this respect, a future goal will be an increment of the amount of guest/host species modifying the experimental conditions. It will also be need to verify the true possible use of cy-[O-(Co-PTPEG$_2$)-O-$CH_2$-]$_4$ as a drug delivery system. In particular, considering the strong affinity of porphyrins toward tumoral tissues, experiments about the host/guest formation with anti-cancer drugs and its successive release will be proved.

## ACKNOWLEDGMENTS

The authors thank the Ministero Istruzione Università e Ricerca (MIUR, Roma) for the partial financial support (PRIN 2008—"*New Porphyrins as Chirogenetic Probes to Recognition of Peptides and Proteins of Biological Interest*"—N. Prot. 2008KHW8K4) and by the project PON01_00074-DIATEME.

## REFERENCES AND NOTES

**1** (a) F. Caruso, R. A. Caruso, H. Mohwald, *Science* **1998,** *282*, 1111–1114; (b) K. Uekama, F. Hirayama, T. Irie. *Chem. Rev.* **1998,** *98*, 2045–2076.

**2** A. D. Bangham, M. M. Standish, J. C. Watkins. *J. Mol. Biol.* **1965,** *13*, 238–252.

**3** D. D. Lasic. *Nature* **1992,** *355*, 279–280.

**4** E. A. Forssen, Z. A. Tökés. *Cancer Res* **1983,** *43*, 546–550.

**5** V. P. Torchilin. *Pharm Res* **2007,** *24*, 1–16.

**6** G. Anneheimherbelin, M. Perreefauvet, A. Gaudemer, P. Helissey, S. Giorgirenault, N. Gresh *N. Tetrahedron Lett.* **1993,** *34*, 7263–7266.

**7** Y. X. Ci, Y. G. Zheng, J. K. Tie; W. B. Chang. *Anal. Chim. Acta.* **1993,** *282*, 695–701.

**8** C. Verchere-Beaur, M. Perree-Fauvet, E. Tarnaud, G. Anneheimherbelin, N. Bone, A. Gaudemer. *Tetrahedron* **1996,** *52*, 13589–13604.

**9** H. J. Schneider, M. X. Wang. *J. Org. Chem.* **1994,** *59*, 7473–7478.

**10** S. A. Priola, A. Raines, W. S. Caughey. *Science* **2000,** *287*, 1503–1506.

**11** W. S. Caughey, L. D. Raymond, M. Horiuchi, B. Caughey. *Proc. Natl. Acad. Sci. USA* **1998,** *95*, 12117–12122.

**12** N. Ono, M. Bouhauchi, K. Maruyama. *Tetrahedron Lett.* **1992,** *33*, 1629–1632.

**13** H. Brunnel, F. Maiterth, B Treittinger. *Chemische Berichte,* **1994,** *127*, 2141–2149.

**14** E. Scamporrino, P. Mineo. *Tetrahedron* **2011,** *67*, 3705–3713.

**15** P. Mineo, E. Scamporrino. *Rapid. Commun. Mass Spectrom.* **1999,** *13*, 2511–2517.

**16** P. Mineo, E. Scamporrino, D. Vitalini, R. Alicata, S. Bazzano. *Rapid. Commun. Mass Spectrom.* **2005,** *19*, 2773–2779.

**17** G. Montaudo, E. Scamporrino, D. Vitalini, P. Mineo. *Rapid. Commun. Mass. Spectrom.* **1996,** *10*, 1551–1559.

**18** D. Vitalini, P. Mineo, E. Scamporrino. *Macromolecules* **1997,** *30*, 5285–5289.

**19** E. Scamporrino, P. Maravigna, D. Vitalini, P. Mineo. *Rapid Commun. Mass Spectrom.* **1998,** *12*, 646–650.

**20** R. G. Little, J. A. Anton, P. A. Loach, J. A. Ibers. *J. Heterocycl. Chem.* **1975,** *12*, 343–349.

**21** V. Villari, P. Mineo, N. Micali; N. Angelini; D. Vitalini; E. Scamporrino. *Nanotechnology* **2007,** *18*, 375503.

**22** V. Villari, P. Mineo, E. Scamporrino, N. Micali. *RSC Adv.* **2012,** *2*, 12989–12998.

**23** V. Villari, P. Mineo, E. Scamporrino, N. Micali. *Chem. Phys.* **2012,** *409*, 23–31.

**24** P. J. Spellane, M. Gouterman, A. Antigas, S. Kim, Y. C. Liu, *Inorg. Chem.* **1980,** *19*, 386.

**25** N. Angelini, N. Micali, P. Mineo, E. Scamporrino, V. Villari; D. Vitalini. *J. Phys. Chem. B* **2005,** *109*, 18645–18651.

**26** P. Mineo, N. Micali, V. Villari, M. G. Donato; E. Scamporrino. *Chem. Eur. J.* **2012,** *18*, 12452–12457.

**27** S. Matile, N. Berova, K. Nakanishi, J. Fleischhauer, R. W. Woody. *J. Am. Chem. Soc.* **1996,** *118*, 5198–5206.

**28** X. Huang, K. Nakanishi, N. Berova. *Chirality* **2000,** *12*, 237–255.